

# Rad51 gain-of-function mutants that exhibit high affinity DNA binding cause DNA damage sensitivity in the absence of Srs2

Punjab S. Malik and Lorraine S. Symington\*

Department of Microbiology, Columbia University Medical Center, New York, NY 10032, USA

Received September 10, 2008; Revised and Accepted September 30, 2008

## ABSTRACT

We previously identified several *rad51* gain-of-function alleles that partially suppress the requirement for *RAD55* and *RAD57* in DNA repair. To gain further insight into the mechanism of action of these alleles, we compared the activities of Rad51-V328A, Rad51-P339S and Rad51-I345T with wild-type Rad51, for DNA binding, filament stability, strand exchange and interaction with the antirecombinase helicase, Srs2. These alleles were chosen because they show the highest activity in suppression of ionizing radiation sensitivity of the *rad57* mutant, and Val 328 and Ile 345 are conserved in the human Rad51 protein. All three mutant proteins exhibited higher affinity for single-stranded DNA (ssDNA) and showed more robust strand exchange activity with oligonucleotide substrates than wild-type Rad51, with the Rad51-I345T and Rad51-V328A proteins displaying higher activity than Rad51-P339S. However, the Srs2 antirecombinase was able to disrupt Rad51-ssDNA complexes formed with all the mutant proteins. *In vivo*, the *rad51-I345T* mutant strain exhibited high resistance to methyl methane sulfonate that was dependent on functional *SRS2*. These results suggest the Srs2 translocase is able to disrupt Rad51-ssDNA complexes at stalled replication forks, but in the absence of Srs2 the enhanced DNA binding of the Rad51-I345T protein is detrimental to cell survival.

## INTRODUCTION

Homologous recombination is an important DNA repair mechanism in mitotic cells and is essential for the accurate segregation of chromosome homologs during meiosis. A central step in homology-dependent repair is the pairing of homologous DNA molecules and exchange of strands to form heteroduplex DNA, a reaction catalyzed by the

RecA/Rad51 family of proteins (1). These proteins form right-handed helical filaments on single-stranded DNA (ssDNA) that is formed by nucleolytic processing of double-strand breaks (DSBs) or at stalled replication forks. The nucleoprotein filament is the active form of the recombinase and is required for the homology search and synapsis with intact double-stranded DNA (dsDNA) leading to strand exchange (1,2).

Human and budding yeast encode two RecA homologs, Rad51 and Dmc1, as well as Rad51-related proteins referred to as the Rad51 paralogs (2). Yeast Rad51 is required for homology-dependent repair in vegetatively growing cells and also for full levels of meiotic recombination and spore formation (3). Dmc1 is only expressed in meiotic cells and is required together with Rad51 for recombination between chromosome homologs (4,5). *Saccharomyces cerevisiae* encodes two Rad51 paralogs, Rad55 and Rad57, that function nonredundantly in spontaneous and DSB-induced recombination (2,6–8). These proteins are thought to function as accessory factors for Rad51 because over-expression of Rad51 can partially suppress the ionizing radiation (IR) sensitivity of *rad55* and *rad57* mutants (9,10). Furthermore, meiosis-specific or IR-induced recruitment of Rad51 to DSBs is greatly reduced in *rad55* and *rad57* mutants (11,12). *In vitro*, the formation of Rad51 filaments on ssDNA is stimulated by replication protein A (RPA), which is thought to allow formation of continuous filaments by removal of secondary structures from ssDNA (13,14). However, addition of RPA prior to Rad51 inhibits filament formation (14–16). The addition of purified Rad55-Rad57 heterodimer to the Rad51-catalyzed strand exchange reaction overcomes the inhibitory effect of RPA, suggesting Rad55-Rad57 promote nucleation of Rad51 onto RPA-coated ssDNA or stabilize Rad51 nucleoprotein filaments (15).

In efforts to understand the function of the yeast Rad51 paralogs, we previously identified gain-of-function alleles of *RAD51* that partially suppress the IR sensitivity of *rad57* mutants (17). The six alleles identified were each shown to have a single amino acid substitution within a 30-amino acid region of Rad51 responsible for the

\*To whom correspondence should be addressed. Tel: +1 212 305 4793; Fax: +1 21 305 1468; Email: lss5@columbia.edu

suppression phenotype. Two of the *rad51* mutants recovered had substitutions of residue Val 328 with either isoleucine or alanine; two different substitutions were identified at Ile 345 (serine or threonine); the other two residues mutated were Pro 339 (to serine) and Gly 359 (to serine). Most of these residues are in the disordered loop 2 (L2) of Rad51, which is thought to correspond to one of the two DNA-binding regions based on cross-linking studies and the recent crystal structure of RecA with ssDNA (18,19). The residue equivalent to Ile 345 is not visible in the *Pyrococcus furiosus* RadA crystal structure, but Thr 345 of the Rad51-I345T protein is the first visible residue after L2 in the Rad51 crystal structure (20,21). Biochemical characterization of the Rad51-I345T mutant protein revealed increased affinity for DNA compared with wild-type Rad51 suggesting the normal function of Rad55-Rad57 is to facilitate nucleation or more stable binding of Rad51 to DNA (17). Val 328 and Ile 345 are both conserved in human Rad51 and mutation of Ile 287 (equivalent to Ile 345 of yeast Rad51) of the human protein to Ser or Thr also confers higher affinity for ssDNA compared with the wild-type protein (22,23). To gain further insight into the mechanism of action of these alleles we have compared the activities of Rad51-V328A, Rad51-P339S and Rad51-I345T with wild-type Rad51, for DNA binding, filament stability, strand exchange and interaction with the antirecombinase helicase, Srs2 (24,25). All three mutant proteins exhibit higher affinity for ssDNA with the Rad51-I345T and Rad51-V328A alleles displaying higher activity than Rad51-P339S. In line with the increased DNA-binding activity, the Rad51-I345T and Rad51-V328A alleles also showed higher strand exchange activity with oligonucleotide substrates. However, none of the proteins was able to withstand the destabilizing effect of Srs2.

## MATERIALS AND METHODS

### Plasmids and yeast strains

Low copy number (pRS413) plasmids expressing the *rad51* gain of function alleles, and the plasmids used to express Rad51 (pEZ3951) and Rad51-I345T in *Escherichia coli* were described previously (17,26). Plasmids to express the Rad51-V328A or Rad51-P339S proteins were created by ligating the 0.95-kb *Bsu36I-BstEII* fragments from pRS413:*rad51-V328A* or pRS413:*rad51-P339S* with *Bsu36I-BstEII* digested pEZ5139. The presence of the mutant alleles was confirmed by DNA sequencing. The plasmid for overexpressing his-tagged Srs2 protein was a kind gift of P. Sung (Yale University).

The yeast strains used in this study are derivatives of W303 (*leu2-3,112 trp1-1 can1-100 ura3-1 ade2-1 his3-11,15*). LSY697 (*MAT $\alpha$  met17-sna ADE2*), LSY991 (*MAT $\alpha$  rad51-I345T rad5-535*) and LSY1405-1A (*MAT $\alpha$  rad51::LEU2 srs2::TRP1*) were described previously (11,17). Strains LSY1791-1B (*MAT $\alpha$  rad51-I345T ADE2*), LSY1827-1D (*MAT $\alpha$  rad51-I345T srs2::HIS3 ADE2*) and LSY1867 (*MAT $\alpha$  srs2::HIS3 ADE2*) were made by standard genetic crosses using stock strains.

### Protein expression and purification

*Saccharomyces cerevisiae* Rad51 and mutant proteins (Rad51-I345T, Rad51-P339S and Rad51-V328A) were overexpressed in *E. coli* strain BL21 (DE3) pLysS (Novagen Inc., Madison, WI, USA) and purified from 10-l cultures as described (26).

For expression and purification of Srs2, *E. coli* BL21 (DE3) pLysS cells were transformed with Pet11c-His<sub>6</sub>-Srs2. The cells (10 l) were initially grown at 37°C and then induced with 0.1 mM IPTG for 18 h at 16°C. After harvesting, the cells were resuspended in 300 ml of breakage buffer [50 mM Tris-Cl, pH 7.4, 600 mM KCl, 10% sucrose, 10 mM EDTA, 1 mM DTT, 0.01% Igepal (Sigma-Aldrich, St Louis, MO, USA)], containing protease inhibitors. The extract was prepared by lysozyme treatment and sonication (Branson Sonifier 250). The extract was clarified by ultracentrifugation (40 000 r.p.m., 2 h) and treated with ammonium sulfate (0.21 g/ml) to precipitate Srs2 and about 15% of the total protein. Following centrifugation, the precipitated protein was dissolved in 200 ml buffer T (25 mM Tris-Cl, pH 7.4, 10% glycerol, 0.5 mM EDTA, 1 mM DTT, 0.01% Igepal) with protease inhibitors. This protein solution was passed through a 60 ml Q Sepharose (GE Healthcare, Piscataway, NJ, USA) column and then loaded onto a 50 ml SP Sepharose (GE Healthcare) column. The SP column was developed with a 500 ml gradient of 200–600 mM KCl in the same buffer without EDTA and DTT (Ni-NTA buffer). Fractions containing Srs2 were pooled and incubated with 3 ml of Ni-NTA agarose (Qiagen, Germantown, MD, USA) for 30 min at 4°C with gentle mixing. The beads were washed with 100 ml of buffer containing 300 mM KCl and 20 mM imidazole. Srs2 was eluted with 300 mM imidazole in Ni-NTA buffer. The Srs2 containing fractions were pooled and dialyzed against T buffer with 200 mM KCl for 2 h. The protein solution was loaded on a high performance SP Sepharose column and eluted with a gradient of 200–600 mM KCl in T buffer. The final Srs2 pool was dialyzed against storage buffer [25 mM Tris-Cl (pH 7.4), 200 mM KCl, 2 mM DTT and 40% glycerol]. Twenty micro liter aliquots of protein were stored at –80°C.

### DNA substrates

Viral (single stranded) and double-stranded replicative forms of  $\phi$ X174, and viral form of M13mp18 were purchased from New England Biolabs, Ipswich, MA, USA. The biotinylated double-stranded trap DNA was PCR amplified using the following primers and ds RF of  $\phi$ X174 as a template:

BIO  $\phi$ X174: 5'Biotin-ACTTTATGCGGACACTTCCTA CAGGTAGCGTTGACCCTAATTTTGGTC-3'  
STEX 130: 5'-TCCGCCAGCAGTCCACTTCGATTTA ATTCGTAACAAGCAGTAGTAATTC-3'

An 80-mer oligonucleotide (STEX-3) was 5'-end labeled using <sup>32</sup>P  $\gamma$ ATP and T4 polynucleotide kinase was used as a substrate for gel mobility shift assays:

5'-CTGCTTTATCAAGATAATTTTTCGACTCATCA GAAATATCCGAAAGTGTTAACTTCTGCGTCATG GAAGCGATAAACTC-3'.

The 5' labeled STEX-3 was annealed with  $\phi$ X174 viral DNA to use as substrate to confirm the Srs2 helicase activity.

#### DNA binding assay

An electrophoretic mobility shift assay (EMSA) was used to analyze the DNA-binding activity of the Rad51 proteins (27). DNA-Rad51 filaments were formed with the indicated amounts of Rad51 protein and 1.5  $\mu$ M nt 5'-[<sup>32</sup>P]-end labeled linear ssDNA (80-nt long) in buffer containing 25 mM HEPES, pH 7.5, 5 mM MgCl<sub>2</sub>, 1 mM DTT, 2.5 mM ATP, 50 mM KCl by incubation at 37°C for 10 min. Glutaraldehyde was then added to a final concentration of 0.125%, incubation continued for 5 min to cross-link protein-DNA complexes, and Tris-HCl (pH 8.0) added to a final concentration of 120 mM to quench the cross-linking reaction. The samples were loaded onto agarose gels (0.9%, 0.5 $\times$  Tris-borate EDTA), and run for 90 min at 80 V (4 V/cm). The DNA in agarose gels was visualized using a PhosphorImager (Amersham Biosciences Typhoon Trio) after drying the gels. The quantification was performed with ImageJ software (National Institutes of Health, Bethesda, MD, USA).

#### Salt titration of protein-DNA complexes

Salt titrations of the protein-DNA complexes were performed by incubating Rad51, Rad51-I345T, Rad51-P339S or Rad51-V328A (1  $\mu$ M) with DNA (1.5  $\mu$ M of 80-nt ssDNA) for 5 min at 37°C. KCl was then added to the indicated final concentrations, and the protein-DNA complexes were incubated for another 5 min at 37°C. The reactions were then fixed with glutaraldehyde (0.125%). Nucleoprotein gel electrophoresis was conducted in 1.0% agarose in TBE buffer for 2 h at 4 V/cm. The dried gels were analyzed by PhosphorImager and quantified using ImageJ software.

#### DNA strand exchange

Rad51 nucleoprotein filaments were formed by incubation Rad51 protein (1.5  $\mu$ M) with ssDNA (9  $\mu$ M nucleotide) in the standard buffer (35 mM Tris-HCl pH 7.4, 2.0 mM ATP, 2.5 mM MgCl<sub>2</sub>, 50 mM KCl, 1 mM DTT, containing an ATP-regenerating system consisting of 20 mM creatine phosphate and 20  $\mu$ g ml<sup>-1</sup> creatine kinase) at 37°C for 5 min (24). DNA strand exchange was initiated by addition of 3  $\mu$ M homologous dsDNA to the nucleoprotein filaments. Spermidine hydrochloride was also added to the reaction at a final concentration of 5 mM. Four micro liter aliquots were withdrawn from the 20  $\mu$ l reaction mixture, deproteinized by the addition of EDTA to 40 mM, SDS to 1.5% and proteinase K to 4.5 mg/ml followed by incubation for 30 min at 37°C, and resolved onto a 15% polyacrylamide gel. The products of DNA strand exchange were visualized using a PhosphorImager.

#### Transfer of Rad51 to bead-bound biotinylated dsDNA

M13mp18 circular (+) strand (6.0  $\mu$ M nucleotides) was incubated for 5 min with Rad51 (1  $\mu$ M) at 37°C, followed

by the addition of Srs2 (5, 10, 20, 40 and 80 nM in a final volume of 20  $\mu$ l of buffer (40 mM Tris-HCl pH 7.4, 2.5 mM ATP, 3.0 mM MgCl<sub>2</sub>, 60 mM KCl, 1 mM DTT, with an ATP-regenerating system consisting of 20 mM creatine phosphate and 20  $\mu$ g ml<sup>-1</sup> creatine kinase) containing 0.01% igeal. After 5 min at 37°C, 4  $\mu$ l of streptavidin beads (Proactive microspheres, Bangs Laboratories, Inc., Fishers, IN, USA) containing 400 ng/ $\mu$ l dsDNA were added to the reaction mixture, followed by mixing for 10 min at 37°C. The beads were captured with low speed centrifugation (4K, 5 min), washed twice with the same buffer and the bound Rad51 was eluted with 20  $\mu$ l of 2% SDS. The supernatant, which contained unbound Rad51, and the SDS eluate (10  $\mu$ l of each) was analyzed by SDS-PAGE. For comparing wild-type Rad51 and Rad51-V328A proteins, the percent of dsDNA bound protein was plotted against the Srs2 concentrations.

#### Methyl methane sulfonate survival assay

Methyl methane sulfonate (MMS) sensitivity of the strains was evaluated by growing strains of the indicated genotype to saturation in rich medium [1% yeast extract; 2% bacto-peptone; 2% dextrose (YPD)], or synthetic complete medium lacking histidine, and then plating aliquots of serially diluted cultures onto solid medium with or without 0.01% MMS. The plates were incubated for 2-3 days at 30°C and then scanned.

## RESULTS

### The Rad51 gain-of-function mutants exhibit increased affinity for ssDNA

We have previously shown that the Rad51-I345T protein has higher affinity for DNA than wild-type Rad51 (17). To test the activity of other gain-of-function alleles, the Rad51-V328A and Rad51-P339S proteins were purified, and their activities compared with Rad51-I345T and wild-type Rad51 (Figure 1A). These alleles were chosen because they map within the putative DNA binding site of Rad51, showed the strongest suppression of the IR sensitivity conferred by *rad57*, and Val328 is conserved in human Rad51. DNA binding was assessed by electrophoretic mobility of glutaraldehyde-fixed Rad51-DNA complexes using an 80-mer ssDNA substrate. Consistent with previous studies, the wild-type Rad51 protein approached maximal binding at a ratio of three nucleotides per Rad51 protomer (Figure 2A). At lower concentrations of Rad51 the mobility of most of the substrate was unchanged. All of the mutant proteins caused maximal retardation of DNA at lower concentrations than observed for the wild-type protein. Similar results were obtained using  $\phi$ X174 viral DNA as substrate (data not shown). Thus, all of the *rad51* gain-of-function alleles tested show higher affinity DNA binding than wild-type Rad51.

To determine the stability of Rad51-ssDNA filaments, a salt titration was performed. Rad51 was incubated with DNA at low salt for 5 min to allow filament formation and the preformed filaments were then challenged with increasing concentrations of KCl, prior to fixation. The salt titration mid point (STMP) was the same for

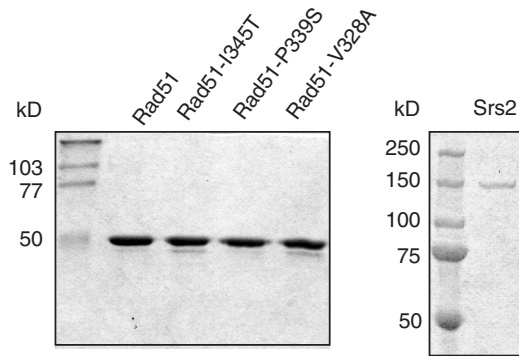


**Figure 1.** Purification of Rad51 and Srs2. Purified Rad51, Rad51-I345T, Rad51-P339S and Rad51-V328A proteins (0.9 μg each) were analyzed by 12% SDS-PAGE and stained with Coomassie blue; the faint faster migrating band is a Rad51 degradation product. Purified Srs2 (0.3 μg) analyzed by 8% SDS-PAGE. The sizes of molecular weight markers are indicated to the left of each panel.

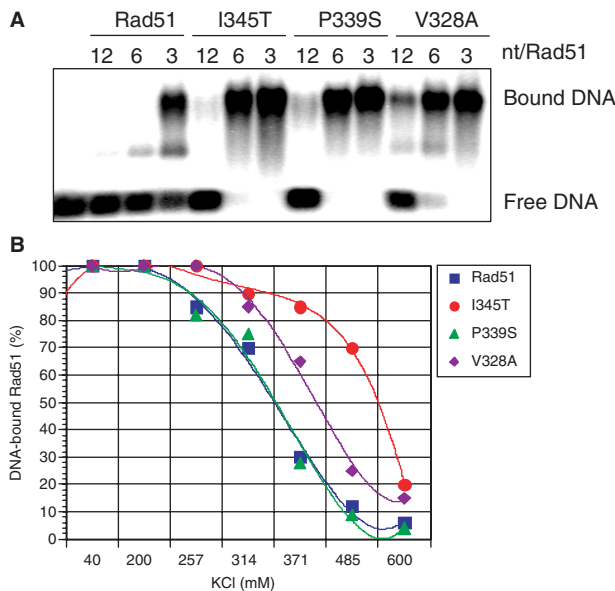


**Figure 2.** DNA binding and stability of Rad51–DNA complexes. (A) Binding of wild-type Rad51 and mutant proteins (Rad51-I345T, Rad51-P339S, Rad51-V328A) to single-stranded oligonucleotide. Reactions containing 5'-end labeled 80-mer oligonucleotide (1.5 μM) incubated with different amounts of Rad51 or mutant proteins at the indicated DNA to protein (nt) ratios at 37°C for 10 min. The nucleoprotein complexes were fixed by the addition of glutaraldehyde to a final concentration of 0.125% and separated from free DNA on a 1% agarose gel. (B) Salt stability of Rad51–ssDNA complexes. The fraction of Rad51-bound DNA was visualized using a PhosphorImager and quantified with ImagaJ software (NIH).

Rad51–ssDNA and Rad51-P339S–ssDNA complexes at 343 mM KCl, whereas the Rad51-V328A and Rad51-I345T mutant protein complexes showed higher stability with STMP values of 407 mM and 542 mM KCl, respectively (Figure 2B). The apparent increased stability could be due to increased on rate or decreased off rate of the mutant proteins at higher salt concentrations. These data support the notion that all of the gain-of-function alleles identified function analogously by increasing the affinity of Rad51 for DNA.

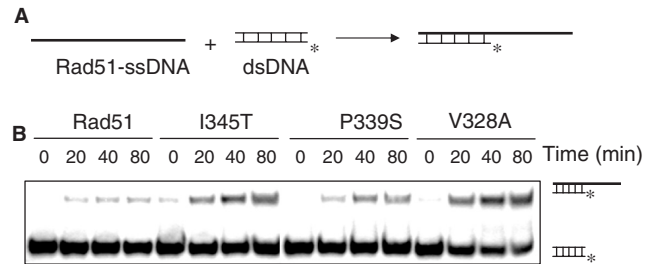


**Figure 3.** Oligonucleotide strand exchange. (A) Schematic diagram of strand exchange assay. <sup>32</sup>P-labeled strand (asterisk). (B) Rad51 (1.5 μM) nucleoprotein filaments were formed on 63-nt long ssDNA substrate (9.0 μM). DNA strand exchange was initiated by addition of <sup>32</sup>P-labeled dsDNA (annealed 31-mers) that was homologous to the 5'-terminal region of 63-nt oligonucleotide.

**DNA strand exchange**

Formation of the Rad51 nucleoprotein filament is essential for homologous pairing and strand exchange. Strand exchange is traditionally measured by exchange of the ssDNA complexed with Rad51 with one strand of a homologous linear duplex DNA. Using long DNA substrates (ϕX174), we observed efficient joint molecule formation by the mutant proteins, but reduced yield of nicked circles indicative of complete strand exchange (data not shown). Mitotic DSB-induced gene conversion tract lengths, which are thought to be a measure of Rad51 strand transfer, are usually <1-kb *in vivo* (28,29). Consequently, we assayed the activity of the mutant proteins using oligonucleotide substrates in which strand exchange proceeds over only 31 bp (Figure 3). The transfer of the 5'-end labeled oligonucleotide from a 31-bp duplex DNA to a homologous 63-nt single-stranded oligonucleotide was monitored by gel electrophoresis (30). The wild-type protein yielded 29% joint molecules at 20 min and the product level did not increase significantly with longer incubation times. The Rad51-I345T and Rad51-V328A proteins supported a more robust reaction yielding 44% and 50% joint molecules, respectively, whereas the strand exchange activity of Rad51-P339S was less than the other hyperactive mutants (37% joint molecules).

**Srs2 destabilizes Rad51–ssDNA filaments**

The Srs2 ATP-dependent translocase/helicase disrupts Rad51–ssDNA filaments *in vitro*, consistent with the *in vivo* function of preventing inappropriate recombination (24,25,31). To determine whether the more stable DNA complexes formed by the Rad51 gain-of-function proteins are more difficult for Srs2 to disrupt, we used the assay illustrated in Figure 4A (24). Rad51 was bound to M13 viral form DNA and then challenged with Srs2 in the presence of a biotinylated dsDNA bound to streptavidin beads to trap displaced Rad51. After a brief incubation, the beads were separated from the reactions by low-speed centrifugation and the amount of Rad51 present on the beads or in the supernatant determined by SDS-PAGE and Coomassie blue staining. As shown previously, Srs2 was able to displace 45% of Rad51 from the ssDNA to be captured by the biotin-bound dsDNA (Figure 4). Srs2 displaced all of the

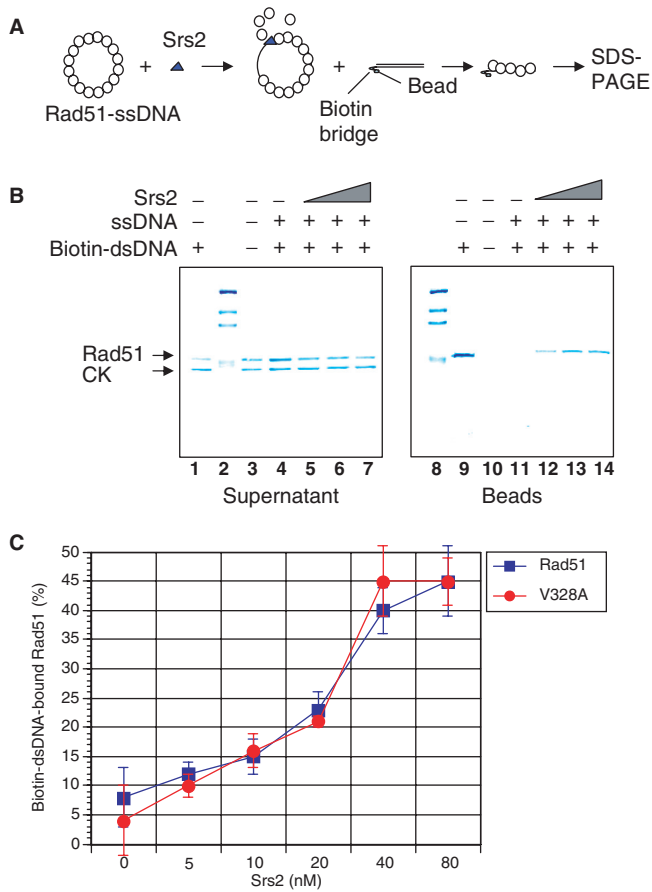


**Figure 4.** Srs2-mediated disruption of presynaptic filaments of Rad51 proteins. (A) Rad51 molecules displaced by Srs2 can be trapped on immobilized DNA duplex attached to streptavidin magnetic beads. (B) Rad51 associated with the magnetic bead-bound duplex was eluted with SDS and analyzed by SDS-PAGE and Coomassie blue staining. (C) Quantitation of Rad51 and Rad51-V328A displacement by Srs2. Creatine kinase (CK) was also present in the supernatant fractions.

mutant proteins to the same extent as wild-type Rad51 (for brevity only Rad51-V328A is shown).

The observation that Srs2 is able to efficiently disrupt Rad51-I345T nucleoprotein filaments may explain the lack of a phenotype for yeast strains with the *rad51-I345T* allele (C.W.Fung and L.S.Symington, unpublished data). To determine whether the increased DNA binding of the Rad51-I345T protein has negative consequences in the absence of Srs2, we tested the sensitivity of a *rad51-I345T srs2* double mutant to MMS. MMS causes replication fork stalling at damaged bases and the resulting single-strand gaps are thought to be substrates for Rad51 to promote lesion bypass by recombination, for fork reversal or for translesion DNA synthesis. The *srs2* single mutant is sensitive to 0.01% MMS as judged by the decrease in colony size, whereas the *rad51-I345T* strain exhibited no sensitivity to MMS (Figure 5A). However, the *rad51-I345T srs2* double mutant exhibited a 4-fold reduction in plating efficiency and greatly reduced colony size in the presence of MMS. To determine whether the enhancement of the MMS sensitivity of the *srs2* mutant by *rad51-I345T* is common to all the *rad51* gain of function alleles, low copy number plasmids

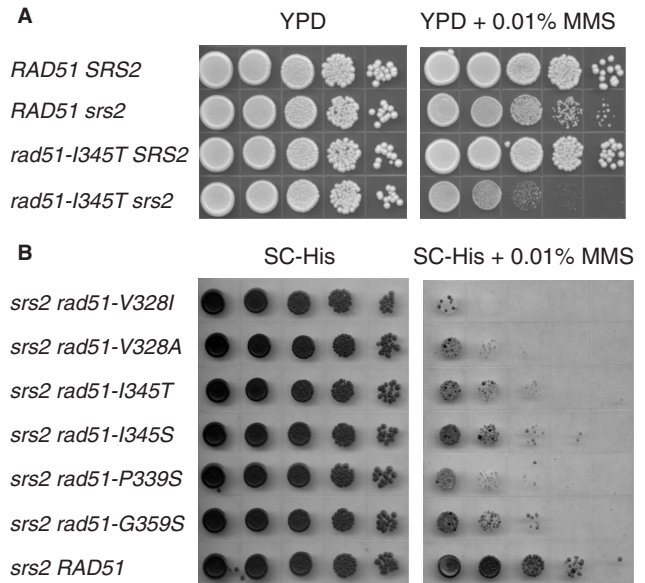


**Figure 5.** The *rad51* gain-of-function alleles cause MMS sensitivity in the absence of Srs2. (A) Ten-fold serial dilutions of the indicated strains were spotted onto YPD plates or YPD containing 0.01% MMS. (B) Plasmids expressing the *rad51* alleles were used to transform a *rad51Δ srs2Δ* strain and the resulting strains serially diluted and spotted onto SC-His plates or SC-His containing 0.01% MMS.

expressing each of the alleles were used to transform a *rad51 srs2* double mutant. We chose to use a *rad51* derivative so that the only allele of *RAD51* expressed in the strain would be the gain of function allele. The plating efficiency of the *rad51 srs2* strain expressing wild-type *RAD51* was reduced 10-fold on medium containing 0.01% MMS, compared with no MMS, however, the plating efficiency of the strain expressing *rad51-I345T* was reduced by an additional 100-fold (Figure 5B). This striking sensitivity to MMS was also observed for the *rad51-V328I* and *rad51-P339S* mutants. The *rad51-I345S* and *rad51-G359S* mutants showed a 10-fold reduction in plating efficiency relative to wild-type, whereas the *rad51-V328I* allele appeared to confer even greater sensitivity to MMS than the *rad51-I345T* allele.

## DISCUSSION

The purpose of this study was to determine whether other *rad51* alleles identified in a genetic screen as suppressors of the IR sensitivity of the *rad57* mutant encode Rad51 variants with higher affinity for ssDNA, as shown previously for the Rad51-I345T protein (17). Of the six alleles identified as *rad57* suppressors, two have substitutions of residue Val 328, two have substitutions at Ile 345 and the other two residues mutated are Pro 339 and Gly 359. Residues Val 328, Pro 339 and Ile 345 are in the L2 region of Rad51. Although there is currently no structure of Rad51 bound to DNA, the recent structure of the RecA-ssDNA complex confirms that residues within the L2 region directly interact with DNA (18). Met 197, Gly 211 and Gly 212 of RecA form hydrogen bonds with the phosphate groups of the nucleotide triplet and the three

stacked bases contact Met 197, Lys 198, Ile199, Gly 200 and Thr 208. Val 328 of ScRad51 corresponds to the residue immediately before Met 197 of RecA, and Ile 345 precedes the conserved pair of glycine residues equivalent to Gly 211 and Gly 212 of RecA. Interestingly, residue 210 in RecA is a threonine and substitution with isoleucine, results in a *recA*-phenotype, whereas substitution with serine does not affect RecA function *in vivo* (32). In the case of Rad51, the residue equivalent to Thr 210 is normally an isoleucine, but substitution with threonine increases DNA binding and subsequent strand exchange activity of the mutant protein. We have not tested the biochemical activity of Rad51-I345S, however, substitution of the equivalent residue with serine in the human Rad51 protein does cause higher affinity DNA binding (23). It is unclear how the conservative substitutions of Val328 influence DNA binding. The biochemical analysis of the Rad51 mutant proteins confirms that suppression of the DSB repair defect of the *rad57* mutant can be achieved by mutations within Rad51 that increase the affinity of the protein for DNA. The increased product yield by the gain-of-function Rad51 mutants in the oligonucleotide strand exchange assay is presumably a consequence of the higher affinity for ssDNA. The failure to detect complete strand exchange products by the gain-of-function Rad51 mutants in the assay utilizing large substrates could be due to Rad51 binding to the displaced strand of the linear duplex and initiation of secondary recombination events to form complex joint molecules.

Although the gain-of-function Rad51 proteins bind ssDNA with higher affinity than wild-type Rad51, the resulting complexes are efficiently disrupted by the Srs2 helicase. This antirecombination activity of Srs2 may explain why the *rad51* gain-of-function alleles confer no apparent phenotype in a *RAD57* background (C.W.Fung and L.S.Symington, unpublished data). However, in the absence of Srs2, the *rad51* gain-of-function alleles confer higher sensitivity to MMS than observed for the *srs2* single mutation. The *srs2 rad51-I345T* double mutant does not exhibit higher sensitivity to IR than the *srs2* single mutant suggesting the synergistic effect is specific for DNA damaging agents that stall DNA synthesis (C.W.Fung and L.S.Symington, unpublished data). MMS causes replication fork stalling and Srs2 is thought to remove Rad51 from ssDNA at stalled replication forks to allow repair to proceed by the error free template-switching branch of postreplication repair or by translesion DNA synthesis instead of recombination (33). Consequently, *srs2* suppresses the MMS sensitivity of *rad6* and *rad18* mutants by channeling lesions to the recombination pathway and *srs2* mutants show elevated rates of spontaneous recombination (31,34,35). In the absence of Srs2, we propose that the Rad51 gain-of-function proteins more effectively compete with other repair proteins that function in lesion bypass, or that other translocases are less efficient at disruption of Rad51–ssDNA complexes formed by the gain-of-function Rad51 proteins. The human Bloom's syndrome helicase (BLM) has been shown to disrupt Rad51–ssDNA complexes *in vitro* (36). Although a similar activity has yet to be reported for Sgs1, the *S. cerevisiae* ortholog of BLM,

*sgs1* mutants exhibit a hyper recombination phenotype and this could possibly be due to a role in disruption of Rad51–ssDNA complexes in addition to the well-characterized function in dissolution of recombination intermediates (37,38). The increased binding of Rad51 to ssDNA at stalled replication forks may cause inappropriate recombination, or block access to the postreplication repair pathways resulting in higher sensitivity to DNA-damaging agents that increase replication fork stalling.

## ACKNOWLEDGEMENTS

We thank C.W. Fung and A.M. Mozlin for helpful discussions and W.K. Holloman for reading the manuscript.

## FUNDING

National Institutes of Health (GM054099 to L.S.S.). Funding for open access charge: GM054099.

*Conflict of interest statement.* None declared.

## REFERENCES

- San Filippo, J., Sung, P. and Klein, H. (2008) Mechanism of eukaryotic homologous recombination. *Annu. Rev. Biochem.*, **77**, 229–257.
- Symington, L.S. (2002) Role of *RAD52* epistasis group genes in homologous recombination and double-strand break repair. *Microbiol. Mol. Biol. Rev.*, **66**, 630–670.
- Shinohara, A., Ogawa, H. and Ogawa, T. (1992) Rad51 protein involved in repair and recombination in *S. cerevisiae* is a RecA-like protein. *Cell*, **69**, 457–470.
- Bishop, D.K., Park, D., Xu, L. and Kleckner, N. (1992) DMC1: a meiosis-specific yeast homolog of *E. coli* recA required for recombination, synaptonemal complex formation, and cell cycle progression. *Cell*, **69**, 439–456.
- Shinohara, A., Gasior, S., Ogawa, T., Kleckner, N. and Bishop, D.K. (1997) *Saccharomyces cerevisiae* recA homologues RAD51 and DMC1 have both distinct and overlapping roles in meiotic recombination. *Genes Cells*, **2**, 615–629.
- Rattray, A.J. and Symington, L.S. (1995) Multiple pathways for homologous recombination in *Saccharomyces cerevisiae*. *Genetics*, **139**, 45–56.
- Mozlin, A.M., Fung, C.W. and Symington, L.S. (2008) Role of the *Saccharomyces cerevisiae* Rad51 paralogs in sister chromatid recombination. *Genetics*, **178**, 113–126.
- Pohl, T.J. and Nickoloff, J.A. (2008) Rad51-independent interchromosomal double-strand break repair by gene conversion requires Rad52 but not Rad55, Rad57, or Dmc1. *Mol. Cell Biol.*, **28**, 897–906.
- Hays, S.L., Firmenich, A.A. and Berg, P. (1995) Complex formation in yeast double-strand break repair: participation of Rad51, Rad52, Rad55, and Rad57 proteins. *Proc. Natl Acad. Sci. USA*, **92**, 6925–6929.
- Johnson, R.D. and Symington, L.S. (1995) Functional differences and interactions among the putative RecA homologs Rad51, Rad55, and Rad57. *Mol. Cell Biol.*, **15**, 4843–4850.
- Fung, C.W., Fortin, G.S., Peterson, S.E. and Symington, L.S. (2006) The rad51-K191R ATPase-defective mutant is impaired for presynaptic filament formation. *Mol. Cell Biol.*, **26**, 9544–9554.
- Gasior, S.L., Wong, A.K., Kora, Y., Shinohara, A. and Bishop, D.K. (1998) Rad52 associates with RPA and functions with rad55 and rad57 to assemble meiotic recombination complexes. *Genes Dev.*, **12**, 2208–2221.
- Sung, P. (1994) Catalysis of ATP-dependent homologous DNA pairing and strand exchange by yeast RAD51 protein. *Science*, **265**, 1241–1243.

14. Sugiyama, T., Zaitseva, E.M. and Kowalczykowski, S.C. (1997) A single-stranded DNA-binding protein is needed for efficient presynaptic complex formation by the *Saccharomyces cerevisiae* Rad51 protein. *J. Biol. Chem.*, **272**, 7940–7945.
15. Sung, P. (1997) Yeast Rad55 and Rad57 proteins form a heterodimer that functions with replication protein A to promote DNA strand exchange by Rad51 recombinase. *Genes Dev.*, **11**, 1111–1121.
16. Sung, P. (1997) Function of yeast Rad52 protein as a mediator between replication protein A and the Rad51 recombinase. *J. Biol. Chem.*, **272**, 28194–28197.
17. Fortin, G.S. and Symington, L.S. (2002) Mutations in yeast Rad51 that partially bypass the requirement for Rad55 and Rad57 in DNA repair by increasing the stability of Rad51-DNA complexes. *EMBO J.*, **21**, 3160–3170.
18. Chen, Z., Yang, H. and Pavletich, N.P. (2008) Mechanism of homologous recombination from the RecA-ssDNA/dsDNA structures. *Nature*, **453**, 489–484.
19. Malkov, V.A. and Camerini-Otero, R.D. (1995) Photocross-links between single-stranded DNA and Escherichia coli RecA protein map to loops L1 (amino acid residues 157-164) and L2 (amino acid residues 195-209). *J. Biol. Chem.*, **270**, 30230–30233.
20. Conway, A.B., Lynch, T.W., Zhang, Y., Fortin, G.S., Fung, C.W., Symington, L.S. and Rice, P.A. (2004) Crystal structure of a Rad51 filament. *Nat. Struct. Mol. Biol.*, **11**, 791–796.
21. Wu, Y., He, Y., Moya, I.A., Qian, X. and Luo, Y. (2004) Crystal structure of archaeal recombinase RADA: a snapshot of its extended conformation. *Mol. Cell*, **15**, 423–435.
22. Davies, O.R. and Pellegrini, L. (2007) Interaction with the BRCA2 C terminus protects RAD51-DNA filaments from disassembly by BRC repeats. *Nat. Struct. Mol. Biol.*, **14**, 475–483.
23. Kurumizaka, H., Aihara, H., Kagawa, W., Shibata, T. and Yokoyama, S. (1999) Human Rad51 amino acid residues required for Rad52 binding. *J. Mol. Biol.*, **291**, 537–548.
24. Krejci, L., Van Komen, S., Li, Y., Villemain, J., Reddy, M.S., Klein, H., Ellenberger, T. and Sung, P. (2003) DNA helicase Srs2 disrupts the Rad51 presynaptic filament. *Nature*, **423**, 305–309.
25. Veaute, X., Jeusset, J., Soustelle, C., Kowalczykowski, S.C., Le Cam, E. and Fabre, F. (2003) The Srs2 helicase prevents recombination by disrupting Rad51 nucleoprotein filaments. *Nature*, **423**, 309–312.
26. Zaitseva, E.M., Zaitsev, E.N. and Kowalczykowski, S.C. (1999) The DNA binding properties of *Saccharomyces cerevisiae* Rad51 protein. *J. Biol. Chem.*, **274**, 2907–2915.
27. Zhang, X.P., Lee, K.I., Solinger, J.A., Kiiantsa, K. and Heyer, W.D. (2005) Gly-103 in the N-terminal domain of *Saccharomyces cerevisiae* Rad51 protein is critical for DNA binding. *J. Biol. Chem.*, **280**, 26303–26311.
28. Nickoloff, J.A., Sweetser, D.B., Clikeman, J.A., Khalsa, G.J. and Wheeler, S.L. (1999) Multiple heterologies increase mitotic double-strand break-induced allelic gene conversion tract lengths in yeast. *Genetics*, **153**, 665–679.
29. Palmer, S., Schildkraut, E., Lazarin, R., Nguyen, J. and Nickoloff, J.A. (2003) Gene conversion tracts in *Saccharomyces cerevisiae* can be extremely short and highly directional. *Nucleic Acids Res.*, **31**, 1164–1173.
30. Mazin, A.V., Zaitseva, E., Sung, P. and Kowalczykowski, S.C. (2000) Tailed duplex DNA is the preferred substrate for Rad51 protein-mediated homologous pairing. *EMBO J.*, **19**, 1148–1156.
31. Rong, L., Palladino, F., Aguilera, A. and Klein, H.L. (1991) The hyper-gene conversion *hpr5-1* mutation of *Saccharomyces cerevisiae* is an allele of the *SRS2/RADH* gene. *Genetics*, **127**, 75–85.
32. Hortnagel, K., Voloshin, O.N., Kinal, H.H., Ma, N., Schaffer-Judge, C. and Camerini-Otero, R.D. (1999) Saturation mutagenesis of the *E. coli* RecA loop L2 homologous DNA pairing region reveals residues essential for recombination and recombinational repair. *J. Mol. Biol.*, **286**, 1097–1106.
33. Pfander, B., Moldovan, G.L., Sacher, M., Hoege, C. and Jentsch, S. (2005) SUMO-modified PCNA recruits Srs2 to prevent recombination during S phase. *Nature*, **436**, 428–433.
34. Robert, T., Dervins, D., Fabre, F. and Gangloff, S. (2006) Mrc1 and Srs2 are major actors in the regulation of spontaneous crossover. *EMBO J.*, **25**, 2837–2846.
35. Schiestl, R.H., Prakash, S. and Prakash, L. (1990) The *SRS2* suppressor of *rad6* mutations of *Saccharomyces cerevisiae* acts by channeling DNA lesions into the *RAD52* DNA repair pathway. *Genetics*, **124**, 817–831.
36. Bugreev, D.V., Yu, X., Egelman, E.H. and Mazin, A.V. (2007) Novel pro- and anti-recombination activities of the Bloom's syndrome helicase. *Genes Dev.*, **21**, 3085–3094.
37. Oh, S.D., Lao, J.P., Hwang, P.Y., Taylor, A.F., Smith, G.R. and Hunter, N. (2007) BLM ortholog, Sgs1, prevents aberrant crossing-over by suppressing formation of multichromatid joint molecules. *Cell*, **130**, 259–272.
38. Wu, L. and Hickson, I.D. (2003) The Bloom's syndrome helicase suppresses crossing over during homologous recombination. *Nature*, **426**, 870–874.